X-ray Absorption Spectroscopic Study of the Temperature and Pressure Dependence of the Electronic Spin States in Several Iron(II) and Cobalt(II) Tris(pyrazolyl)borate Complexes

Cécile Hannay

Institut de Chimie, B6, Université de Liège, B-4000 Liège 1, Belgium

Marie-Jeanne Hubin-Franskin

Directeur de Recherches, FNRS, Institut de Chimie, B6, Université de Liège, B-4000 Liège 1, Belgium

Fernande Grandjean

Institut de Physique, B5, Université de Liège, B-4000 Sart-Tilman, Belgium

Valérie Briois, Jean-Paul Itié, and Alain Polian

Laboratoire pour l'Utilisation du Rayonnement Electromagnétique, Université de Paris Sud, F-91405 Orsay, France

Swiatoslaw Trofimenko

Department of Chemistry and Biochemistry, University of Delaware, Newark, Delaware 19716

Gary J. Long*

Department of Chemistry, University of Missouri−Rolla, Rolla, Missouri 65409-0010

Received May 1, 1997[⊗]

An iron and cobalt K-edge X-ray absorption study has been undertaken, at 295 and 77 K, to investigate the electronic spin states of Fe[HB(pz)$_3$]$_2$, **1**, Fe[HB(3,5-(CH$_3$)$_2$pz)$_3$]$_2$, **2**, Fe[HB(3,4,5-(CH$_3$)$_3$pz)$_3$]$_2$, **3**, Co[HB(pz)$_3$]$_2$, **4**, Co[HB(3,5-(CH$_3$)$_2$pz)$_3$]$_2$, **5**, and Co[HB(3,4,5-(CH$_3$)$_3$pz)$_3$]$_2$, **6**, where pz is the 1-pyrazolyl moiety. Between 295 and 77 K complex **2** shows a spin-state crossover whereas **1** and **3**−**6** remain low-spin and high-spin, respectively. The spectra show a clear difference, in both the relative intensities and the relative energies, of the metal 1s to 4p electronic transition in the high-spin and the low-spin states. An analogous study of Fe[HB(pz)$_3$]$_2$, **1**, between 295 and 450 K reveals that it undergoes a gradual reversible spin-state crossover to the high-spin state above ca. 360 K. The high-pressure room-temperature XANES spectra of **1** indicate that it remains low-spin between ambient pressure and 90 kbar, whereas complex **2** shows the expected spin-state crossover between zero and ca. 30 kbar and is low-spin between 40 and 90 kbar. The three cobalt complexes are gradually converted from the high-spin to the low-spin state with increasing pressure, complex **4** showing the least spin-state change and complex **6** showing the most change. The energies of the metal 4p virtual orbitals are found to be very sensitive to pressure and to the electronic spin state of the metal. An EXAFS analysis for the cobalt complexes indicates both that they are all structurally very similar, with the expected high-spin cobalt to nitrogen bond lengths, and that they remain high-spin upon cooling from 295 to 77 K.

Introduction

The octahedral and pseudooctahedral coordination complexes of iron(II) have long provided the classic and well-studied examples of the high-spin, low-spin, and spin-crossover compounds for the 3d^6 electronic configuration.[1] This is fortunate for the goal of this work, which is the study of the spin crossover in cobalt(II) complexes as a function of temperature and pressure. Such studies, especially at high pressure, are more difficult with cobalt(II) complexes than with iron(II) complexes mainly because the latter can be rather easily studied by the Mössbauer effect at high pressure. Thus, in order to facilitate our X-ray absorption spectral investigation of several cobalt(II) complexes at high pressure, we have undertaken a parallel study of the analogous iron(II) complexes whose electronic properties are well understood. In this way the XANES and EXAFS results for the iron(II) complexes serve as a template to understand the high-pressure electronic properties of the cobalt(II) complexes.

In an octahedral complex, there is a critical crystal field below which iron(II) has the $t_{2g}^4e_g^2$, $^5T_{2g}$, high-spin ground state electronic configuration and above which it has the t_{2g}^6, $^1A_{1g}$, low-spin ground state electronic configuration. Moreover, if the crystal field experienced by the iron(II) is of the same order

[⊗] Abstract published in *Advance ACS Abstracts,* November 1, 1997.

(1) Gütlich, P. In *Mössbauer Spectroscopy Applied to Inorganic Chemistry*; Long, G. J., Ed.; Plenum: New York, 1984; Vol. 1, p 287.

S0020-1669(97)00506-5 CCC: $14.00

of magnitude as the critical field (i.e., the crystal field splitting energy, 10*Dq*, is similar to the mean electron pairing energy, ρ), the complex may show a spin-state transformation, usually a spin crossover for an iron(II) complex, between the two electronic configurations.[1,2] In this case, the crystal field may increase sufficiently under an external perturbation, such as the lattice contraction with decreasing temperature[3−8] or increasing external pressure[9−13] to produce a spin-state crossover. Similar spin-state transitions are also found in the octahedral complexes of metal ions with the $3d^4$, $3d^5$, and $3d^7$ ground state electronic configurations.[14] It is also possible to induce a photochemical spin transition using light-induced excited state spin trapping,[15] or to study the susceptibility of the transient excited paramagnetic state,[16] or to study ligand-driven light-induced spin changes.[17]

Coordination complexes containing various substituted poly(1-pyrazolyl)borate ligands[18] have been very useful in investigating the spin-state transitions in various transition metal complexes. The iron(II) complexes formed with the hydrotris(1-pyrazolyl)borate ligand and its 3,5-dimethyl and 3,4,5-trimethyl derivatives, $Fe[HB(pz)_3]_2$, **1**, $Fe[HB(3,5\text{-}(CH_3)_2pz)_3]_2$, **2**, and $Fe[HB(3,4,5\text{-}(CH_3)_3pz)_3]_2$, **3**, have been the subject of several Mössbauer spectral studies as a function of temperature and pressure.[3,9,19,20] The room-temperature single-crystal X-ray structures of **1** and **2** are known.[21] The average metal−ligand Fe−N bond distances are 1.973 Å for **1** and 2.172 Å for **2**. The spin state is responsible for a 10% change in the average Fe−N distance.

Upon cooling, the crystal field strengths of these three ligands yield different spin-state behaviors. $Fe[HB(pz)_3]_2$, **1**, exhibits a photoelectron spectrum[22] which is consistent with the high-spin state above 400 K, whereas a variety of techniques indicate that it exhibits a gradual spin crossover beginning below 400 K and is low-spin at lower temperatures.[3] $Fe[HB(3,5\text{-}(CH_3)_2pz)_3]_2$, **2**, shows[20] a relatively sharp spin crossover from high-spin above 195 K to low-spin below 195 K, whereas, in contrast, $Fe[HB(3,4,5\text{-}(CH_3)_3pz)_3]_2$, **3**, is high-spin at 293 K and shows[9] no spin crossover upon cooling to 1.7 K.

At room temperature and 78 kbar applied pressure, the Mössbauer spectra of $Fe[HB(pz)_3]_2$, **1**, show the presence of ca. 20% of a high-spin component.[9] This behavior is rather unexpected but has been observed previously by Drickamer and co-workers[23−25] in the Mössbauer spectra of several iron(II) complexes at high pressure. For $Fe[HB(3,5\text{-}(CH_3)_2pz)_3]_2$, **2**, at room temperature, only ca. 4−5 kbar is required to convert 50% of the complex from high-spin to low-spin. In contrast, for $Fe[HB(3,4,5\text{-}(CH_3)_3pz)_3]_2$, **3**, 46 kbar is required to convert 50% of the complex from high-spin to low-spin.[9]

Less is known about the electronic spin-state properties of $Co[HB(pz)_3]_2$, **4**, $Co[HB(3,5\text{-}(CH_3)_2pz)_3]_2$, **5**, and $Co[HB(3,4,5\text{-}(CH_3)_3pz)_3]_2$, **6**, although previous NMR work[18,26] indicates they are high-spin at room temperature, a conclusion that is consistent with the cobalt−nitrogen bond lengths observed in the single-crystal structure[27,28] and the photoelectron spectrum[22] of **4**. To our knowledge the crystal structures of **5** and **6** have not been determined nor have any of these complexes been studied at high pressure.

The purpose of this paper is to present an X-ray absorption spectral study of $Fe[HB(pz)_3]_2$, **1**, $Fe[HB(3,5\text{-}(CH_3)_2pz)_3]_2$, **2**, $Fe[HB(3,4,5\text{-}(CH_3)_3pz)_3]_2$, **3**, $Co[HB(pz)_3]_2$, **4**, $Co[HB(3,5\text{-}(CH_3)_2pz)_3]_2$, **5**, and $Co[HB(3,4,5\text{-}(CH_3)_3pz)_3]_2$, **6**, at 295 and 77 K. In addition, we have measured at 295 K the X-ray absorption spectra of **1**, **2**, **4**, **5**, and **6** at the K-edge of iron or cobalt at several pressures between ambient and 90 kbar. X-ray absorption spectroscopy is ideally suited to follow the spin crossover because it is sensitive to both the electronic structure and the local structure around an atom. Not only can the XANES spectra be used to follow the electronic modification occurring during spin crossover, but an EXAFS analysis can also provide information about the contraction of the first coordination shell around the metal upon transition from the high-spin to the low-spin state. The temperature studies were initiated to determine the electronic spin states of the complexes, especially the cobalt complexes, and to determine to what extent the XANES spectra reflect the influence of the spin-state changes on the empty states just above the Fermi level. The pressure studies were initiated to better understand the surprising partial conversion of **1** to the high-spin state at high pressure.[9] Moreover, extended X-ray absorption fine structure, EXAFS, studies provide new structural information on all of these compounds.

Experimental Section

Samples of **1**−**6** were prepared by standard literature methods.[20,26]

The X-ray absorption spectra were recorded with the synchrotron radiation provided by the DCI storage ring at the Laboratoire pour l'Utilisation du Rayonnement Electromagnétique, Université de Paris Sud, France. The synchrotron radiation was produced by a storage ring operated with 1.85 GeV positrons and with an average beam intensity of ca. 300 mA. The 295 and 77 K and the high-temperature measurements were performed with the EXAFS III spectrometer which

(2) Gütlich, P.; Hauser, A.; Spiering, H. *Angew. Chem., Int. Ed. Engl.* **1994**, *33*, 2024.
(3) Grandjean, F.; Long, G. J.; Hutchinson, B. B.; Ohlhausen, L.; Neill, P.; Holcomb, J. D. *Inorg. Chem.* **1989**, *28*, 4406.
(4) Cartier dit Moulin, C.; Rudolf, P.; Flank, A.-M.; Chen, C.-T. *J. Phys. Chem.* **1992**, *96*, 6196.
(5) Cartier dit Moulin, C.; Sainctavit, P.; Briois V. *Jpn. J. Appl. Phys.* **1993**, *32*, Suppl. 32-2, 38.
(6) Briois, V.; Cartier dit Moulin, C.; Momenteau, M.; Maillard, P.; Zarembowitch, J.; Dartyge, E.; Fontaine, A.; Tourillon, G.; Thuéry, P.; Verdaguer, M. *J. Chim. Phys.* **1989**, *86*, 1623.
(7) Young, N. A. *J. Chem. Soc., Dalton Trans.* **1996**, 1275.
(8) Real, J.-A.; Gallois, B.; Granier, T.; Suez-Panama, F.; Zarembowitch, J. *Inorg. Chem.* **1992**, *31*, 4972.
(9) Long, G. J.; Hutchinson, B. B. *Inorg. Chem.* **1987**, *26*, 608.
(10) Pebler, J. *Inorg. Chem.* **1983**, *22*, 4125.
(11) Roux, C.; Zarembowitch, J.; Itié, J.-P.; Verdaguer, M.; Dartyge, E.; Fontaine, A.; Tolentino, H. *Inorg. Chem.* **1991**, *30*, 3174.
(12) Roux, C.; Adams, D. M.; Itié, J.-P.; Polian, A.; Hendrickson, D. N.; Verdaguer, M. *Inorg. Chem.* **1996**, *35*, 2846.
(13) McCusker, J. K.; Zvagulis, M.; Drickamer, H. G.; Hendrickson, D. N. *Inorg. Chem.* **1989**, *28*, 1380.
(14) Martin, R. L.; White, A. H. In *Transition Metal Chemistry*; Carlin, R. L., Ed.; Dekker: New York, 1968; Vol. 4, p 113.
(15) Poganiuch, P.; Gütlich, P.; Hasselbach, K. M.; Hauser, A.; Spiering, H. *Inorg. Chem.* **1987**, *26*, 455.
(16) Addison, A. W.; Burman, S.; Wahlgren, C. G.; Rajan, O. A.; Rowe, T. M.; Sinn, E. *J. Chem. Soc., Dalton Trans.* **1987**, 2621.
(17) Roux, C.; Zarembowitch, J.; Gallois, B.; Granier, T.; Claude, R. *Inorg. Chem.* **1990**, *33*, 2273.
(18) Trofimenko, S. *Chem. Rev.* **1993**, *93*, 943.
(19) Jesson, J. P.; Trofimenko, S.; Eaton, D. R. *J. Am. Chem. Soc.* **1967**, *89*, 3158.
(20) Jesson, J. P.; Weiher, J. F.; Trofimenko, S. *J. Chem. Phys.* **1968**, *48*, 2058.
(21) Oliver, J. D.; Mullica, D. F.; Hutchinson, B. B.; Milligan, W. O. *Inorg. Chem.* **1980**, *19*, 165.
(22) Bruno, G.; Centineo, G.; Ciliberto, E.; Di Bella, S.; Fragala, I. *Inorg. Chem.* **1984**, *23*, 1832.
(23) Fung, S. C.; Drickamer, H. G. *J. Chem. Phys.* **1969**, *51*, 4353.
(24) Fisher, D. C.; Drickamer, H. G. *J. Chem. Phys.* **1971**, *54*, 4825.
(25) Bargeron, C. B.; Drickamer, H. G. *J. Chem. Phys.* **1971**, *55*, 3471.
(26) Jesson, J. P.; Trofimenko, S.; Eaton, D. R. *J. Am. Chem. Soc.* **1967**, *89*, 3148. Trofimenko, S. *J. Am. Chem. Soc.* **1967**, *89*, 3170.
(27) Churchill, M. R.; Gold, K.; Maw, C. E., Jr. *Inorg. Chem.* **1970**, *9*, 1597.
(28) The indication in ref 27 that compound **4** has the low-spin, $S = {}^1/_2$, spin multiplicity is in error and the correct spin state is high-spin with $S = {}^3/_2$.

Table 1. Relative Energies[a] and Intensities of the XANES Transitions

compound	*T*, K		P	B	C	D	M	E
$Fe[HB(pz)_3]_2$, **1**	450	energy	1.3	9.7	16.5	27.7		60.0
		intensity	0.04	0.51	1.61	1.16		1.13
	295	energy	1.2	8.6	18.8	27.8	39.8	75.7
		intensity	0.03	0.29	1.61	1.35	1.01	1.14
	77	energy	1.2	8.6	18.4	28.3	39.6	75.9
		intensity	0.03	0.30	1.66	1.38	1.02	1.14
$Fe[HB(3,5\text{-}(CH_3)_2pz)_3]_2$, **2**	295	energy	1.2	9.5	16.1	26.4	36.1	58.0
		intensity	0.02	0.60	1.78	1.11	0.88	1.16
	77	energy	0.5	8.9	17.1	27.3	36.6	62.0
		intensity	0.03	0.41	1.63	1.24	1.01	1.14
$Fe[HB(3,4,5\text{-}(CH_3)_3pz)_3]_2$, **3**	295	energy	1.5	9.5	16.2	26.4	36.4	58.1
		intensity	0.03	0.61	1.73	1.10	0.88	1.15
	77	energy	1.2	9.5	16.4	26.4	36.1	59.1
		intensity	0.03	0.54	1.69	1.15	0.92	1.14
$Co[HB(pz)_3]_2$, **4**	295	energy	2.0	12.8	17.1	22.0, 26.8		58.5
		intensity	0.03	0.90	1.79	1.40, 1.14		1.18
	77	energy	2.2	12.8	17.2	21.7, 27.6		58.6
		intensity	0.03	0.89	1.85	1.42, 1.12		1.20
$Co[HB(3,5\text{-}(CH_3)_2pz)_3]_2$, **5**	295	energy	2.2	12.7	17.4	26.4	38.1	59.1
		intensity	0.03	0.91	1.76	1.15	0.87	1.17
	77	energy	2.2	12.8	17.3	26.4	38.4	58.8
		intensity	0.02	0.92	1.79	1.14	0.87	1.18
$Co[HB(3,4,5\text{-}(CH_3)_3pz)_3]_2$, **6**	295	energy	2.2	12.8	17.3	27.1	37.6	59.1
		intensity	0.03	0.92	1.68	1.11	0.88	1.16
	77	energy	2.0	12.8	17.3	27.0	37.8	59.0
		intensity	0.02	0.91	1.74	1.12	0.88	1.18

[a] The absorption energies in eV relative to the 7112 eV K-edge of iron foil or the 7709 eV K-edge of cobalt foil. The accuracy of the C absorption line is ± 0.25 eV, the P and B lines ± 0.5 eV, the D and E lines ± 0.75 eV, and the M line ± 1 eV.

uses a double-crystal silicon (311) monochromator. The measurements were carried out in the transmission mode with ionization chambers in front and in back of the absorber. A pellet of the compound, with an area of 1 cm^2 and a mass of ca. 30 mg, was pressed. The EXAFS spectra were recorded with a 2 eV step and with a 1 s accumulation time per step over a 1000 eV energy range. The XANES spectra were recorded with a 0.25 eV step over a 125 eV energy range. The spectrum of an iron or cobalt foil was recorded periodically to check the energy calibration, and the first derivative of the iron foil K-edge spectrum at 7112 eV or the cobalt foil K-edge spectrum at 7709 eV was used to define the zero-energy reference point. The measurements at 77 K were made in a liquid nitrogen cryostat. The high-temperature spectra of **1** were obtained in a furnace, whose temperature was proportionally controlled to prevent overheating and thermal oscillation. The temperature was allowed to stabilize for ca. 10 min after each heating and cooling step. The relative temperatures are believed to be accurate to ±2 K whereas the absolute temperature is accurate to ±10 K. Because of the volatility of **1** at higher temperatures, its was not studied above 450 K.

The high-pressure XANES measurements were performed[29] at room temperature in a diamond anvil cell with copper−beryllium gaskets which had been preindented to a pressure of 40 kbar. The measurements were carried out on a dispersive-mode spectrometer which uses dispersive X-ray optics consisting of a bent crystal of silicon (111) acting as a polychromator and a position-sensitive detector, a system which reduces the data acquisition time. The pressure was determined by following the shift of the ruby fluorescence line of small ruby chips added to the sample and excited by an argon laser.

Results and Discussion

In the following sections, the analysis of the spectra of the iron(II) complexes, **1**−**3**, whose electronic properties are rather well established even at high pressure,[3,9] is discussed first because it serves as the basis for the analysis of the spectra obtained for the cobalt(II) complexes, **4**−**6**. We have found that this approach is especially useful in the analysis of the high-pressure spectra of the cobalt(II) complexes, for which no previous studies of the spin crossover with increasing pressure are available. Further, the detailed multiple-scattering analysis of the near-edge spectra of the complexes is very dependent upon knowing the single-crystal X-ray structure in both spin states, a requirement which is met for the iron(II) complexes[21] but not for the cobalt(II) complexes.

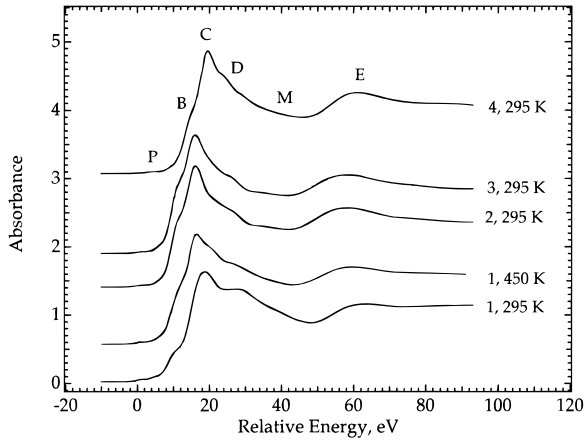

Figure 1. XANES spectra of $Fe[HB(pz)_3]_2$, **1**, $Fe[HB(3,5\text{-}(CH_3)_2pz)_3]_2$, **2**, $Fe[HB(3,4,5\text{-}(CH_3)_3pz)_3]_2$, **3**, and $Co[HB(pz)_3]_2$, **4**, measured at 450, 295, or 77 K, as indicated. The zero of the energy scale is given relative to 7112 and 7709 eV, the K-edges of iron and cobalt foil, respectively.

XANES Spectra: Temperature Dependence. The X-ray absorption near-edge structure spectra, the XANES spectra, of $Fe[HB(pz)_3]_2$, **1**, $Fe[HB(3,5\text{-}(CH_3)_2pz)_3]_2$, **2**, $Fe[HB(3,4,5\text{-}(CH_3)_3pz)_3]_2$, **3**, and $Co[HB(pz)_3]_2$, **4**, are shown in Figure 1, which also shows the designations of the different observed absorption features. The absorbance of these spectra has been normalized by using the intersection point between the background and the first EXAFS oscillation as unit absorbance. For clarity, the individual spectra in Figure 1 are shifted upward by a constant amount of absorbance. The 77 K XANES spectra for **1** and **3** are virtually the same as those obtained at room temperature and hence are not shown in Figure 1. The spectra of $Co[HB(pz)_3]_2$, **4**, at 77 K and the spectra of $Co[HB(3,5\text{-}(CH_3)_2pz)_3]_2$, **5**, and $Co[HB(3,4,5\text{-}(CH_3)_3pz)_3]_2$, **6**, at both 295 and 77 K are

(29) Itié, J.-P.; Baudelet, F.; Dartyge, E.; Fontaine, A.; Tolentino, H.; San Miguel, A. *High Pressure Res.* **1992**, *8*, 697.

virtually identical in appearance to that of $Co[HB(pz)_3]_2$, **4**, shown in Figure 1, and thus are not shown. The relative energies and normalized intensities of the XANES absorptions are given in Table 1. The XANES spectra of **1** and **2** were reported very recently by Zamponi et al.,[30] but as will be noted below, there are small differences between their spectra and the spectra reported herein, differences which probably are due to differences in resolution. Further, as will be discussed below, we make assignments completely different from those proposed by Zamponi et al.[30]

The interpretation of the edge structure in the XANES spectra is not simple, and a detailed analysis of the absorption profiles shown in Figure 1 requires a complete multiple-scattering analysis, which will be given in a future paper.[31] However, in conjunction with the known structures of the compounds, first-approximation assignments of the absorption peaks below or in the rising edge can be made with a one-electron model based on electronic dipole transitions. The room-temperature single-crystal X-ray studies[21,27] have shown that **1**, **2**, and **4** are pseudooctahedral coordination complexes in which the six nitrogen atoms coordinated to the iron(II) or cobalt(II) produce a small but not exact distortion from O_h toward D_{3d} symmetry at the iron or cobalt ion.

In ligand field theory, the electrostatic field produced by the ligands of octahedral complexes removes the 5-fold degeneracy of the metal 3d orbitals into one 3-fold degenerate set of nonbonding or slightly antibonding t_{2g}* orbitals and one set of 2-fold degenerate e_g* antibonding orbitals. The small reduction in symmetry below octahedral symmetry[21,27] in complexes **1**, **2**, and **4**, and presumably in the remaining complexes reported herein, removes to a small extent the degeneracy of both the 3d metal t_{2g}* and e_g* antibonding orbitals and the metal 4p empty orbitals, but the extent of the splitting of these orbitals will be small in the case of the complexes studied herein. Notice that in these complexes the 3d states are strongly localized, roughly atomic, whereas the 4p states are highly delocalized and their description has to take into account the bonded near neighbors. More important, the reduction in symmetry will permit the mixing of the 3d and 4p metal atomic orbitals into molecular orbitals of mixed character. With this distortion and mixing in mind, it is possible to make electronic assignments.

The very weak "pre-edge" absorption peaks, labeled P in Figure 1, are clearly assigned to the transition of the 1s electron to the iron or cobalt 3d orbitals. The intensity of this line is very small because it formally involves an electronic dipole transition which is angular momentum forbidden with $\Delta l = 2$. When the metal is located in a noncentrosymmetric site, such as in a tetrahedral complex, extensive molecular orbital mixing of the metal 3d orbitals with the metal 4p orbitals occurs, thus making the 1s to 3d−4p mixed orbital transition angular momentum allowed. This mixing is known to be more extensive in tetrahedral than in pseudooctahedral complexes and to increase as the coordination number decreases.[6,32] A pre-edge absorption, P, has been observed in several pseudotetrahedral substituted (pyrazolyl)borate complexes.[33] When the metal is located in a centrosymmetric site, no 4p and 3d mixing occurs, and theoretically no preedge absorption should be observed. However, some relaxation of the dipole selection rule, such as by quadrupole allowed-transitions,[34,35] can occur and account for the existence of small pre-edge features even in centrosymmetric complexes. Of course, small distortions from idealized centrosymmetric symmetry can also lead to the appearance of such weak pre-edge absorptions, as is the case for the iron and cobalt complexes investigated herein. As shown in Figure 1, the pre-edge absorption, P, is present in both the high-spin and low-spin complexes. This pre-edge peak, although probably present in the XANES spectra of **1** and **2** and definitely present in the spectra of the related iron(III) complexes, is ignored in the assignment presented by Zamponi et al.[30] Relative to the Fermi level in iron and cobalt metal, the energy of P is only ca. 0.9 eV higher in the cobalt(II) complexes than in the iron(II) complexes, probably as a consequence of the higher electronegativity[36] in the former case.

The first strong absorption, B, occurs as a shoulder on the low-energy side of the absorption edge and is observed in *all* of the complexes studied herein, as is clearly indicated by a distinct peak in the first-derivative plots of all the spectra. This shoulder typically has one-third to one-half the intensity of the subsequent peak, C, the most intense peak in the spectrum. Similar shoulders have been observed in the XANES spectra of a variety of iron(II) complexes.[7,30,37,38] Because of its high intensity, shoulder B must be asssigned to a metal 1s to 4p transition, a dipole-allowed transition. Because this shoulder can be reproduced by one-electron full multiple-scattering calculations,[31] we assume that ligand to metal shake-down transitions, which have been proposed to interpret such structures in iron(II) porphyrin complexes,[39] play little if any role in the assignment of the transitions associated with shoulder B. In the absence of any "shake-down" contribution, the energy of shoulder B, and hence the energies of the three metal 4p orbitals, are ca. 7.4 and 8.2 eV above P in the high-spin and low-spin iron complexes, respectively. In the high-spin cobalt complexes the average value is ca. 10.6 eV above P or ca. 3.2 eV above that of the high-spin iron(II) complexes. The analogous energies in the gaseous iron(II) and cobalt(II) free ions are 10.2 and 12.3 eV, respectively, for a difference of 2.1 eV.[40] Thus, although the 3d to 4p orbital energy difference in the complexes is, as expected, lower than that in the free ions as a result of the ligand field, the difference between the iron(II) and cobalt(II) complexes, i.e., 3.2 eV, is larger than the 2.1 eV difference found in the free ions.[40] This difference no doubt arises as a result of the differing metal−ligand covalency in the complexes with the two metals, complexes which have rather longer metal−nitrogen bond lengths in the case of the high-spin iron complexes; see below.

Rather strangely, Zamponi et al.[30] do not observe the shoulder, B, in the spectrum of **2** but do observe it in the spectrum of **1** and, in spite of its high intensity, assign this shoulder to the forbidden 1s to 3d transition, an assignment we cannot accept,

(30) Zamponi, S.; Gambini, G.; Conti, P.; Gioia Lobbia, G.; Marassi, R.; Berrettoni, M.; Cecchi, P. *Polyhedron* **1995**, *14*, 1929.
(31) Briois, V.; Hannay, C.; Hubin-Franskin, M.-J.; Grandjean, F.; Long, G. J.; Trofimenko, S.; Sainctavit, P.; Itié, J. P.; Polian, A. *Inorg. Chem.*, in preparation.
(32) Roe, A. L.; Schneider, D. J.; Mayer, R. J.; Pyrz, J. W.; Windom, J.; Que, L. *J. Am. Chem. Soc.* **1984**, *106*, 1676. Randall, C. R.; Shu, L.; Chiou, Y.-M.; Hagen, K. S.; Ito, M.; Kitajima, N.; Lachicotte, R. J.; Zang, Y.; Que, L. *Inorg. Chem.* **1995**, *34*, 1036.
(33) Hannay, C.; Thissen, R.; Briois, V.; Hubin-Franskin, M.-J.; Grandjean, F.; Long, G. J.; Trofimenko, S. *Inorg. Chem.* **1994**, *33*, 5983.
(34) Hahn, J. E.; Scott, R. A.; Hodgson, K. O.; Doniach, S.; Desjardins, S. R.; Solomon, E. I. *Chem. Phys. Lett.* **1982**, *88*, 595.
(35) Pichering, I. J.; George, G. N. *Inorg. Chem.* **1995**, *34*, 3142.
(36) Huheey, J. E.; Keiter, E. A.; Keiter, R. L. *Inorganic Chemistry: Principles of Structure and Reactivity*, 4th ed.; HarperCollins: New York, 1993; p 188.
(37) Briois, V.; Cartier dit Moulin, C.; Sainctavit, P.; Brouder, C.; Flank, A.-M. *J. Am. Chem. Soc.* **1995**, *117*, 1019.
(38) Chen, L. X.; Wang, Z.; Burdett, J. K.; Montano, M. A.; Norris, J. R. *J. Chem. Phys.* **1995**, *99*, 7958.
(39) Cartier, C.; Momenteau, M.; Dartyge, E.; Fontaine, A.; Tourillon, G.; Michalowicz, A.; Verdaguer, M. *J. Chem. Soc., Dalton Trans.* **1992**, 609.
(40) Moore, C. E. *Atomic Energy Levels*; National Bureau of Standards: Washington, DC, 1952; Vol. II, pp 60−61, 86.

especially in the view of the presence of the pre-edge peak, P, in all of our spectra and in the spectra of Zamponi et al.[30]

Multiple electron-scattering processes are responsible for peak C and shoulders D and M on the high-energy side of the absorption edge, as has been noted earlier[39] and as is indicated by a full multiple-scattering calculation,[31] based on the single-crystal X-ray structures[21,27] of complexes **1**, **2**, and **4**. In this work it was found that the XANES spectrum calculated in the framework of multiple scattering processes within the coordination complex gave a result rather similar to that observed in Figure 1. Indeed, excellent agreement with the observed spectrum was obtained[31] if 33 atoms, the metal, the 6 coordinated nitrogen atoms, 6 noncoordinated nitrogen atoms, 18 of the pyrazolyl carbon atoms, and 2 of the boron atoms, all within ca. 5 Å of the metal, were included in the multiple-scattering calculations. An alternate assignment of peak C to one or two of the 4p states split by the low-symmetry crystal field is unrealistic because of the large energy difference between shoulder B and peak C, a difference which is far too large to have resulted from the small observed distortion from octahedral symmetry found in these complexes.[21,27]

Finally, we note that the shape and energy of absorption E are characteristic of the spin state of the absorbing atom. This absorption is at the frontier of the XANES and EXAFS regions and, for such molecular systems, is mainly determined by scattering processes inside the first coordination shell.[37] Its energy is very much dependent on the metal to near-neighbor nitrogen bond lengths. The energies of peak E verify the Natoli rule,[41] which states that, for a given symmetry, the peak positions and shell distances are given by $Ed^2 =$ constant, where E is the peak energy relative to a given zero energy and d is the mean bond length, in this case the metal to nitrogen bond length. The longer bond lengths in the high-spin complexes correspond to a lower energy of ca. 58−59 eV, whereas the shorter bond lengths in the low-spin complexes correspond to a higher energy. The determination of this energy is not easy in the case of low-spin complexes because the absorption is broad with two apparent maxima at ca. 63 and 88 eV. Natoli's rule would yield an absorption at ca. 70 eV, which is between the energies of the two maxima.

Earlier work[3] has shown that the low-spin complex, Fe[HB(pz)$_3$]$_2$, **1**, undergoes a gradual transition to the high-spin state upon heating above room temperature, a transition which was found to show a very large hysteresis when carried out on rather large unground or crushed crystals of the complex. Thus, we have measured the XANES spectra of complex **1** both upon heating to 450 K and upon subsequent cooling. The resulting spectra are shown in Figure 2A and reveal the expected change from the low-spin state at 295 K to the high-spin state at 450 K. In order to simulate the percentage of high-spin state as a function of temperature above 295 K, we have taken weighted linear combinations of the low-spin spectrum of complex **1**, obtained at 295 K, and the high-spin spectrum of complex **2**, also obtained at 295 K, and adjusted the percentage composition to give the best agreement with the observed spectra. The results of this simulation are shown in Figure 2B, and a comparison of Figure 2A and Figure 2B reveals an excellent agreement between the simulations and the observed spectra. The resulting percentage of the high-spin state is shown in Figure 3 for a heating and cooling cycle. Although some hysteresis is observed in the spin transition, it is much smaller than that observed previously[3] because in the current work it was necessary to grind the sample before measuring the XANES spectra. The associated EXAFS results are discussed below.

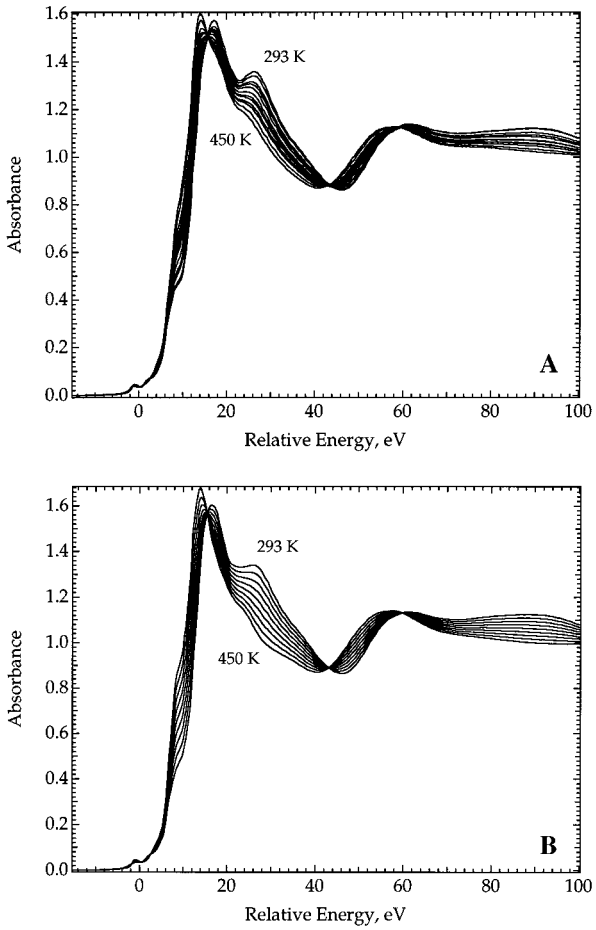

Figure 2. (A) XANES spectra of Fe[HB(pz)$_3$]$_2$, **1**, measured as a function of temperature at various temperatures between 295 K, the highest curve at 30 eV, and 450 K, the lowest curve at 30 eV. The zero of the energy scale is given relative to 7112 eV, the K-edge of iron foil. (B) Simulation of the XANES spectra of Fe[HB(pz)$_3$]$_2$, **1**, as a function of temperature at various temperatures between 295 K, the highest curve at 30 eV, and 450 K, the lowest curve at 30 eV, obtained by taking weighted linear combinations of the 295 K low-spin spectrum of complex **1** and the 295 K high-spin spectrum of complex **2**. The zero of the energy scale is given relative to 7112 eV, the K-edge of iron foil.

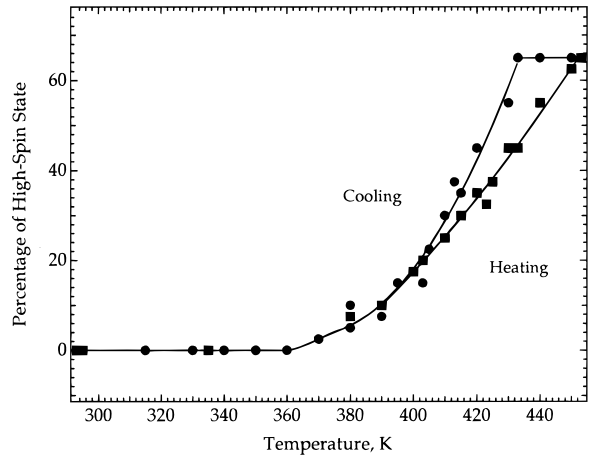

Figure 3. Percentage of high-spin Fe[HB(pz)$_3$]$_2$, **1**, as a function of temperature upon heating, ■, and cooling, ●, as determined from the XANES results.

XANES Spectra: Pressure Dependence. The room-temperature XANES spectra of Fe[HB(pz)$_3$]$_2$, **1**, measured at the various indicated pressures are shown in Figure 4. As expected, the 0 kbar spectrum of **1**, obtained in the diamond anvil cell

(41) Natoli, C. R.; Benfatto, M.; Doniach, S. *Phys. Rev. A* **1986**, *34*, 4682.

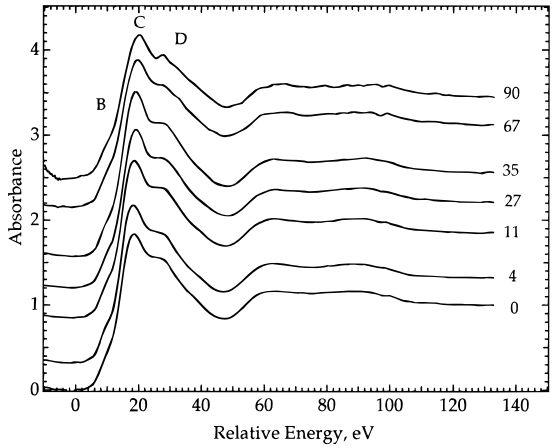

Figure 4. XANES spectra of Fe[HB(pz)$_3$]$_2$, **1**, measured at the pressures indicated in kbar. The zero of the energy scale is given relative to 7112 eV, the K-edge of iron foil.

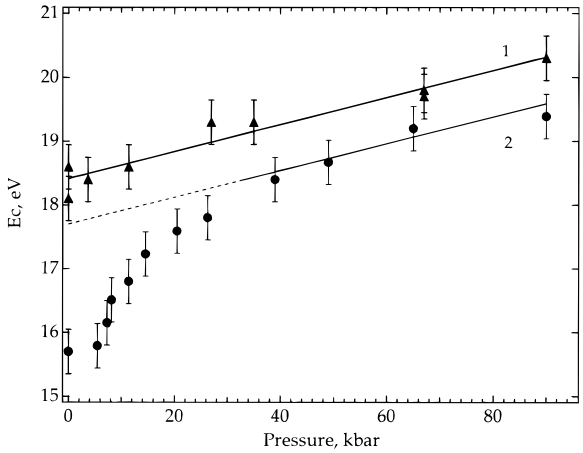

Figure 5. Room-temperature pressure dependence of the energy of peak C in the XANES spectra of Fe[HB(pz)$_3$]$_2$, **1**, and Fe[HB(3,5-(CH$_3$)$_2$pz)$_3$]$_2$, **2**.

and shown in Figure 4, is virtually the same as that shown in Figure 1. At first glance, there appears to be little if any change in the XANES spectra of **1** with increasing pressure. This is especially true in the EXAFS scattering region above ca. 50 eV in relative energy, the region in which the scattering should be very sensitive to the iron(II) to nitrogen near-neighbor bond length. Thus, it would appear that there is no indication of the presence of the high-spin form of complex **1** at high pressure. Earlier Mössbauer spectral studies[9] have revealed that as much as 15 and 22% of the high-spin form of complex **1** is present at 45 and 78 kbar, respectively. Unfortunately, this unusual spin-state transition, from low-spin to high-spin with increasing pressure, does not appear to be reflected in the XANES spectra shown in Figure 4. Although the signal to noise ratio of the spectrum may decrease because of a change in thickness of the samples, the sensitivity of the technique remains at better than ca. 10% as is evidenced by the results on the high-spin to low-spin transitions. The first derivatives of the spectra shown in Figure 4, between 0 and 40 eV, do indicate some small, but significant, shifts in peaks B and C, but not D, energy shifts which increase with increasing pressure. It should be noted that the generation of any low-spin component at high pressure would, of course, cause shifts in the opposite direction; see Figure 1. The pressure dependence of the energy of peak C is shown in Figure 5. The increase in energy with increasing pressure is linear with a slope of 0.021 eV/kbar and a zero-pressure intercept of 18.4 eV, a value which agrees well with the 18.8 eV value reported in Table 1 at ambient pressure. The

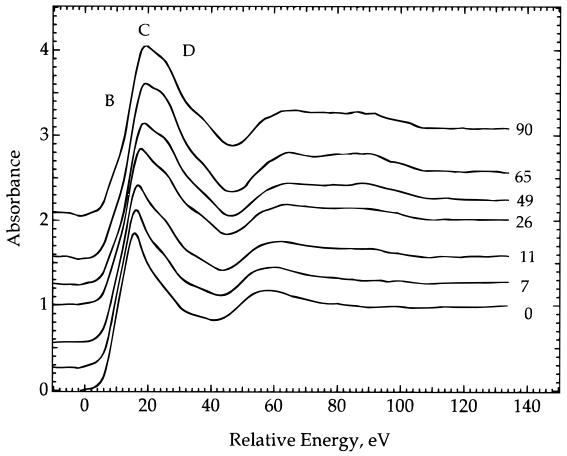

Figure 6. XANES spectra of Fe[HB(3,5-(CH$_3$)$_2$pz)$_3$]$_2$, **2**, measured at 295 K and the pressures indicated in kbar. The zero of the energy scale is given relative to 7112 eV, the K-edge of iron foil.

increase in the energy of peak C with pressure, shown in Figure 5, indicates a pressure sensitivity of the energy difference between the iron 1s orbital and the multiple-scattering peaks[31] observed for the iron(II) complexes. The energy of shoulder B, and thus the iron 4p orbitals, also shows a similar pressure sensitivity. A similar shift of the XANES absorption peaks to higher energies with increasing pressure has been observed for isotropically compressible materials as a result of decreasing bond lengths.[42]

The room-temperature XANES spectra of Fe[HB(3,5-(CH$_3$)$_2$-pz)$_3$]$_2$, **2**, measured at the various indicated pressures, are shown in Figure 6. As expected, the 0 kbar spectrum of **2**, obtained in the diamond anvil cell and shown in Figure 6, is virtually the same as the room-temperature spectrum shown in Figure 1. In contrast to the case of complex **1**, for complex **2** there are substantial changes in the XANES spectra with increasing pressure. First, in the EXAFS scattering region, above ca. 40 eV in relative energy, both peak E and the subsequent peak shift to higher energy with pressure as the electronic ground state of **2** changes from high-spin to low-spin and the iron(II) to nitrogen bond lengths decrease. These shifts clearly indicate the change with pressure of the electronic spin state, as has been observed[9] in the Mössbauer spectra of complex **2**. In the XANES region of the spectra, shown in Figure 6, although the resolution is poorer than at ambient pressure, there appears to be an increase of ca. 3−5 eV with increasing pressure in the relative energy of peaks B, C, and D, as well as a substantial increase in the relative intensity of peak D. These rather large increases clearly reflect both the change in the spin multiplicity of the ground state with an increase in crystal field strength from the increasing pressure and the inherent pressure sensitivity of the iron(II) 1s to 4p electronic transition, as was previously observed in **1**. More specifically, the pressure dependence of the energy of peak C of **2** is shown in Figure 5. Below ca. 30 kbar, there is a dramatic increase in the energy of peak C. At 40 kbar, **2** is completely low-spin and there is no additional change in the spectrum with additional increases in the pressure, except for the linear energy shift due to the pressure sensitivity of the 1s to 4p transition. This behavior is in excellent agreement with high-pressure Mössbauer spectral results,[9] which show dramatic changes in the electronic spin state below 30 kbar and little change above 30 kbar. The lines in Figure 5 indicate that, above ca. 30 kbar, the pressure dependence of the energy of peak C of the low-spin form of complex **2** is

(42) San Miguel, A.; Polian, A.; Gauthier, M.; Itié, J.-P. *Phys. Rev. B* **1993**, *48*, 8683.

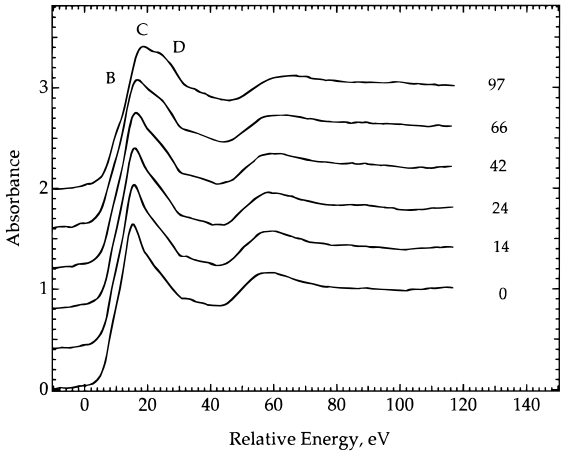

Figure 7. XANES spectra of Co[HB(3,5-$(CH_3)_2$pz)$_3$]$_2$, **5**, measured at 295 K and the pressures indicated in kbar. The zero of the energy scale is given relative to 7709 eV, the K-edge of cobalt foil.

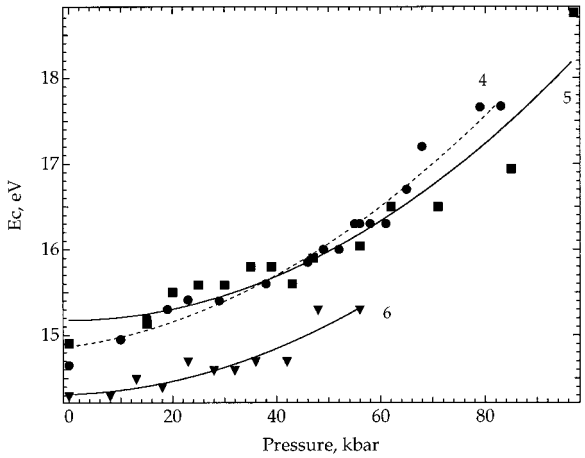

Figure 8. Room-temperature pressure dependence of the energy of peak C in the XANES spectra of Co[HB(pz)$_3$]$_2$, **4**, Co[HB(3,5-$(CH_3)_2$pz)$_3$]$_2$, **5**, and Co[HB(3,4,5-$(CH_3)_3$pz)$_3$]$_2$, **6**.

virtually the same as for low-spin complex **1**, but with a zero-pressure intercept of 17.7 eV, a value which is 0.7 eV lower than the 18.4 eV value found for complex **1**.

The 295 K pressure dependence of the XANES spectra of Co[HB(3,5-$(CH_3)_2$pz)$_3$]$_2$, **5**, is shown in Figure 7. Very similar results are obtained for compounds **4** and **6**, which are not shown herein. The first step in the analysis of the cobalt spectra at high pressure has been to determine the pressure dependence of the energy of peak C, E_C; see Figure 8. Clearly, the results are very different from those shown in Figure 5 and indicate that the cobalt complexes respond differently to pressure than either **1**, which remains low-spin at high pressure, or **2**, which shows a spin-state transition between 0 and ca. 40 kbar. From Figure 8 it is apparent that the electronic spin states of the cobalt complexes change gradually with increasing pressure, a change which is consistent with the above observation that they remain high-spin upon cooling from 295 to 77 K. The absence of a sharp, cooperative spin-state crossover in the cobalt complexes is no doubt responsible for this difference.

In order to better understand the differences between the iron and cobalt complexes under pressure, it is useful to use more than just the energy of peak C. By using the entire XANES spectral absorption profile, a profile which is much more sensitive to the electronic spin-state changes, we have been able to determine the percentage change in the electronic spin states of complexes **2**, **4**, **5**, and **6**, with pressure; see Figure 9.

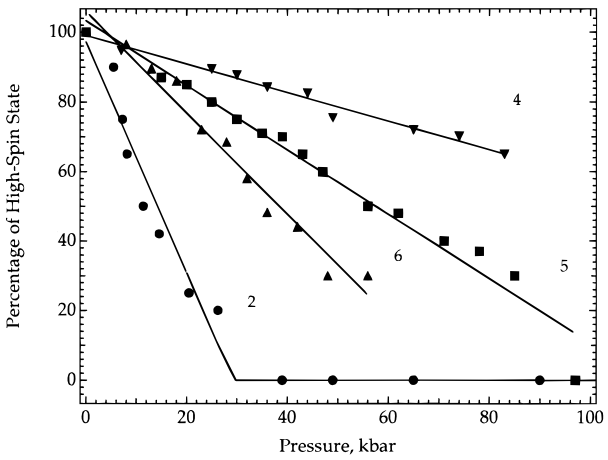

Figure 9. 295 K pressure dependence of the percentage of the high-spin state in Fe[HB(3,5-$(CH_3)_2$pz)$_3$]$_2$, **2**, Co[HB(pz)$_3$]$_2$, **4**, Co[HB(3,5-$(CH_3)_2$pz)$_3$]$_2$, **5**, and Co[HB(3,4,5-$(CH_3)_3$pz)$_3$]$_2$, **6**.

The percentage change in spin state shown in Figure 9 for complex **2** has been obtained by taking a linear combination of its spectrum observed at 40 kbar, which is assumed to be completely low-spin, as no more change occurs above 40 kbar, and its spectrum observed at ambient pressure, which is completely high-spin. However, because of the pressure-induced shift in the spectrum (see Figure 5), it is necessary, when taking the linear combination, to shift the high-pressure spectrum to lower energy by the amount given by the slope shown in Figure 5. As expected, the results shown for complex **2** in Figure 9 are very similar to those observed in the earlier high-pressure Mössbauer spectral study.[9]

For the cobalt complexes **4**−**6**, a similar procedure was used except that, in these cases, it was not possible to assume that the high-pressure cobalt spectra were completely in the low-spin state, because at the highest pressure there were still changes occurring in the spectra. Thus, in these cases, a linear combination of the high-spin ambient-pressure spectra of **4**−**6** and the low-spin 40 kbar spectrum of **2** was used to profile the highest pressure cobalt spectra measured. This approach was surprisingly successful in reproducing the high-pressure spectral profile for complexes **4**−**6** and indicated that, at the highest pressures studied, the complexes were 35, 100, and 70% in the electronic low-spin state, respectively. The resulting highest pressure profile was then used, in linear combination with the ambient-pressure spectra, to obtain the percentage contribution of the low-spin state to each of the spectra measured at intermediate pressures. The results, shown in Figure 9, indicate that the cobalt complexes respond differently to pressure than does complex **2**, an iron complex which shows a clear spin-state crossover with decreasing temperature.[9] It would appear that there is no sharp spin-state crossover in the case of the cobalt complexes, but rather a more gradual, virtually linear conversion from the high-spin state at ambient pressure to the low-spin state at high pressure.

If there was a direct analogy between the electronic spin state changes in the cobalt complexes and those in the iron complexes,[3,9] we would anticipate that Co[HB(pz)$_3$]$_2$, **4**, would be the most readily converted to the low-spin state with pressure, whereas Co[HB(3,4,5-$(CH_3)_3$pz)$_3$]$_2$, **6**, would be the least readily converted. Exactly the opposite is the case, as is indicated in Figure 9. As will be noted below (see Table 2), the EXAFS analysis yields virtually the same cobalt to nitrogen bond lengths in all three complexes, **4**−**6**, at 295 and 77 K, a distance which is between that of the iron to nitrogen bond lengths in the high-spin and low-spin iron(II) complexes. Thus it would appear

Table 2. EXAFS Analysis of the Iron and Cobalt K-edge Spectra[a]

compound	*T*, K	metal−nitrogen bond length, Å	Debye−Waller factor, Å	Γ,[b] Å^{-2}	quality factor, %
Fe[HB(pz)$_3$]$_2$, **1**	295	1.97	0.061	0.60	0.61
	77	1.97	0.052	0.60	0.57
Fe[HB(3,5-(CH$_3$)$_2$pz)$_3$]$_2$, **2**	295	2.17	0.093	0.63	1.14
	77	1.98	0.055	0.70	1.87
Fe[HB(3,4,5-(CH$_3$)$_3$pz)$_3$]$_2$, **3**	295	2.17	0.096	0.62	1.18
	77	2.17	0.071	0.59	1.11
Co[HB(pz)$_3$]$_2$, **4**	295	2.12	0.080	0.64	0.75
	77	2.12	0.064	0.61	0.74
Co[HB(3,5-(CH$_3$)$_2$pz)$_3$]$_2$, **5**	295	2.12	0.083	0.65	0.42
	77	2.12	0.060	0.65	0.58
Co[HB(3,4,5-(CH$_3$)$_3$pz)$_3$]$_2$, **6**	295	2.13	0.095	0.65	2.39
	77	2.12	0.069	0.65	0.19

[a] The bond lengths are accurate to ±0.02 Å, and the Debye−Waller factors are accurate to ±0.005 Å. [b] Γ is related to the electron mean free path by the relationship $\lambda(k) = k/T$.

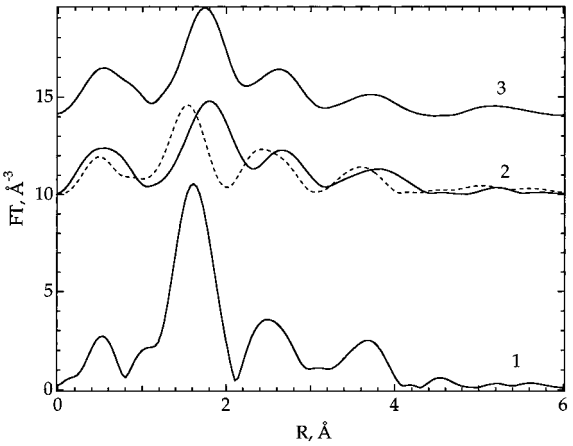

Figure 10. Fourier transforms of the EXAFS scattering for Fe[HB(pz)$_3$]$_2$, **1**, Fe[HB(3,5-(CH$_3$)$_2$pz)$_3$]$_2$, **2**, and Fe[HB(3,4,5-(CH$_3$)$_3$pz)$_3$]$_2$, **3**, measured at 295 K, solid lines, or 77 K, broken line.

that the changes with pressure in the cobalt complexes may be more closely related to the nature of the substituents on the pyrazolyl moiety. Co[HB(pz)$_3$]$_2$, **4**, with no methyl substituents, shows the least change in spin state with pressure, whereas Co[HB(3,4,5-(CH$_3$)$_3$pz)$_3$]$_2$, **6**,with three methyl substituents, shows the most change. Apparently the added flexibility of the methyl groups permits the cobalt to nitrogen bond length to decrease with pressure more effectively, thus promoting the low-spin state. Unfortunately it is not possible at LURE to measure the EXAFS spectra at high pressure, and thus we do not know how the bond lengths respond to pressure at this time. Future planned work at high pressure at other synchrotron facilities may permit such studies.

EXAFS Analysis. An EXAFS analysis of the X-ray scattering, to an energy of ca. 1000 eV above the iron or cobalt K-edge absorption, has been carried out, and the Fourier transforms of this scattering for the iron complexes, **1**−**3**, are shown in Figure 10. The transforms for the analogous cobalt complexes, **4**−**6**, are virtually identical to that of complex **3**, illustrated in this figure, and thus are not shown. Examination of these transforms clearly reveals the expected differences for the low-spin complex, **1**, the high-spin complex, **3**, and the spin-state crossover with temperature in complex **2**. The structural parameters resulting from simulations of the EXAFS scattering, based initially on the known X-ray structures[21,27] of **1**, **2**, and **4**, are given in Table 2. In each case, the subsequent refinement of the scattering model leads to a coordination number of 6 for the metal and to metal−nitrogen bond lengths which are either virtually identical to those obtained from the single-crystal X-ray structural studies or consistent with those expected of high-spin, or in the case of **2** at low temperature, low-spin complexes. Except for those of **2**, perhaps because the bond lengths are only determined in this analysis to ca. ±0.02 Å, the bond lengths decrease very little upon cooling from 295 to 77 K. The resulting bond lengths for the three cobalt complexes are all very similar and clearly indicate that they remain high-spin upon cooling to 77 K.

The Debye−Waller factors of 0.061 and 0.093 Å, obtained at 295 K from the EXAFS analysis (see Table 2) for Fe[HB(pz)$_3$]$_2$, **1**, and Fe[HB(3,5-(CH$_3$)$_2$pz)$_3$]$_2$, **2**, respectively, are very similar to the values of 0.062 and 0.083 Å obtained from the thermal factors reported in the X-ray structural study[21] of these complexes. In contrast, the Debye−Waller factor of 0.080 Å, obtained at 295 K for Co[HB(pz)$_3$]$_2$, **4**, is larger than the 0.058 Å value obtained from the X-ray structure thermal parameters.[27] However, it should be noted that the 0.080 Å value is very similar to those obtained herein for the other high-spin metal complexes. In all cases, the Debye−Waller factors, as expected, decrease upon cooling, decreases which range from 20 to 28% for complexes **3**−**6**, the complexes which remain high-spin upon cooling. In contrast, the decrease is smaller at 15% for complex **1**, which remains low-spin upon cooling, and much larger at 41% for complex **2**, which changes from high-spin at 295 K to low-spin at 77 K, with a simultaneous decrease of 0.19 Å, or 9% in the iron to nitrogen bond lengths. It is interesting that cobalt complexes **5** and **6** exhibit Debye−Waller factor decreases of 27 and 28%, respectively, whereas complex **4** shows only a 20% decrease. It appears that the extra flexibility associated with the two or three additional methyl groups in the former complexes permits a larger decrease in their Debye−Waller factors.

Because compound **1** undergoes a spin crossover above room temperature, the EXAFS results obtained above room temperature were analyzed as a mixture of a low-spin state with a metal to ligand distance of 1.97 Å and a high-spin state with a metal to ligand distance of 2.17 Å. In this analysis, compounds **1** and **2** at 295 K, the structures of which are known,[21] have been chosen as model compounds for the low-spin and high-spin states, respectively, and the experimental phases and amplitudes extracted from their 295 K EXAFS results were used in the analysis of the high-temperature EXAFS results obtained on compound **1**. Within the constraint of a coordination number of 6 for the metal, the percentages of low-spin and high-spin states and the Debye−Waller factors for both spin states were refined. The results of these refinements, the quality factors of which are less than 1% and hence are excellent, are given in Table 3.

The temperature dependence of the percentage of the high-spin state in **1** is shown in Figure 11. The increase in high-

Table 3. EXAFS Analysis for $Fe[HB(pz)_3]_2$, **1**, between 295 and 450 K

	low-spin state		high-spin state		
T, K	percentage	Debye−Waller factor, Å	percentage	Debye−Waller factor, Å	quality factor, %
295	100	0.053	0		0.10
430[a]	52	0.064	48	0.100	0.06
450[a]	35	0.067	65	0.104	0.10
410[b]	67	0.062	33	0.092	0.02
400[b]	78	0.061	22	0.089	0.04
380[b]	91	0.062	9	0.085	0.02
360[b]	98	0.063	2	0.080	0.07
340[b]	100	0.062	0		0.10
293[b]	100	0.055	0		0.10
380[c]	91	0.062	9	0.086	0.02
390[c]	87	0.064	13	0.083	0.03
400[c]	81	0.065	19	0.094	0.02
410[c]	74	0.065	26	0.095	0.03
420[c]	65	0.063	35	0.095	0.03
450[c]	37	0.067	63	0.099	0.20

[a] Initial heating. [b] Initial cooling. [c] Second heating.

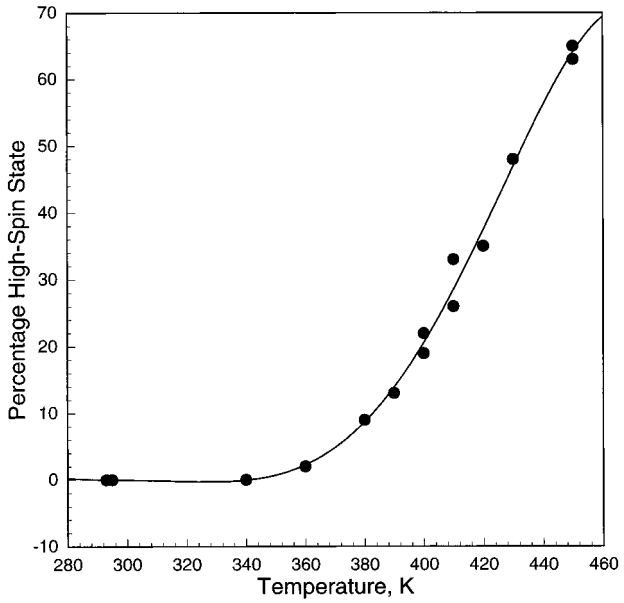

Figure 11. Percentage of high-spin $Fe[HB(pz)_3]_2$, **1**, as a function of temperature, as determined from the EXAFS results.

spin percentage with increasing temperature is similar to that shown in Figure 3. However, the ca. ±1% accuracy of the percentage values given in Table 3 and shown in Figure 11 is better than the ca. ±3% accuracy in Figure 3. In contrast with Figure 3, Figure 11 does not show any hysteresis, presumably because the compound has been finely ground to prepare the absorber for the high-temperature EXAFS study.

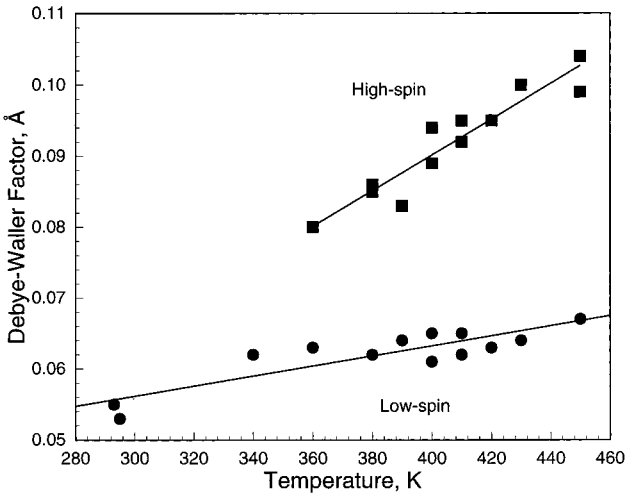

Figure 12. Debye−Waller factors for the low-spin, ●, and the high-spin, ■, fractions of $Fe[HB(pz)_3]_2$, **1**, as a function of temperature.

In conclusion, both the XANES and the EXAFS results obtained for $Fe[HB(pz)_3]_2$, **1**, between 295 and 450 K reveal the presence of a progressive spin crossover from a low-spin to a high-spin state, a crossover which starts at 360 K and leads to 65% of the high-spin state at 450 K. The hysteresis of this spin crossover is very sensitive to the preparation of the sample.[3] The sample prepared from small crystals for the Mössbauer experiments shows the largest hysteresis, and the finely ground powdered sample used for the EXAFS measurements shows no hysteresis.

The temperature dependence of the Debye−Waller factors for the low-spin and high-spin states of compound **1** is shown in Figure 12. As expected, both factors increase linearly with temperature. The Debye−Waller factor for the high-spin state shows a slope of 2.51×10^{-4} Å/K, which is, larger than that of the low-spin state, which is 7.07×10^{-5} Å/K. Also, as expected, at all temperatures, the Debye−Waller factor for the high-spin state is larger than that of the low-spin state. A similar difference is observed in Table 2 for compound **2**.

Acknowledgment. The authors acknowledge, with thanks, the support obtained from the Ministère de la Communauté Française de Belgique under ARC Grant 94/99-175, the Fonds National de la Recherche Scientifique, Belgium, and the Division of Materials Research of the U.S. National Science Foundation under Grant DMR-9521739. M.-J.H.-F. thanks the Fonds National de la Recherche Scientifique, Belgium, for a position of Directeur de Recherches.

IC970506R